Biophysical Characterization of the Interactions of HTI-286 with Tubulin Heterodimer and Microtubules

Girija Krishnamurthy,*,‡ Wendy Cheng,‡ Mei-Chu Lo,‡ Ann Aulabaugh,‡ Vladimir Razinkov,‡ WeiDong Ding,‡ Frank Loganzo,§ Arie Zask,|| and George Ellestad‡

Biophysics/Enzymology, Screening Sciences, Oncology Research, and Chemical Sciences, Wyeth Research, Pearl River, New York 10965

Received August 26, 2003; Revised Manuscript Received September 25, 2003

ABSTRACT: HTI-286 is a synthetic analogue of the natural product hemiasterlin and is a potent antimitotic agent. HTI-286 inhibits the proliferation of tumor cells during mitosis. The observed antimitotic activity is due to the binding of HTI-286 to tubulin. This report details the effects of HTI-286 on soluble tubulin and preassembled microtubules. HTI-286 binds tubulin monomer and oligomerizes it to an 18.5 S species corresponding to a discrete ring structure consisting of about 13 tubulin units as determined by sedimentation equilibrium analyses. The rate of formation of the oligomers is dependent on the concentration of HTI-286 and the time of incubation. Tubulin oligomers, specifically the 18.5 S species, form slowly. The interactions of HTI-286 with tubulin were studied by isothermal titration calorimetry. HTI-286 binds tubulin rapidly, and the initial association of HTI-286 with tubulin is enthalpically driven with a ΔH value of −14 kcal/mol at 25 °C and a dissociation constant of ca. 100 nM. However, the accompanying tubulin oligomerization event does not produce measurable heats at 25 °C. The dissociation constant estimated from the changes in the intrinsic fluorescence of tubulin was found to be consistent with the calorimetric results. Both HTI-286 and hemiasterlin bind tubulin with nearly equal potency. However, the stability of the tubulin oligomers is not identical under size-exclusion column chromatographic conditions. The tubulin oligomers formed in the presence of HTI-286 dissociate on the column, while the corresponding oligomers formed in the presence of hemiasterlin are stable. Tubulin undergoes a change in the secondary structure in the presence of HTI-286, which is evidenced by changes in the circular dichroic absorption spectrum of tubulin. In contrast to the microtubule-stabilizing effects of paclitaxel, both HTI-286 and hemiasterlin depolymerize preassembled microtubules at micromolar concentrations.

Tubulin is a major target for anticancer agents that act by interfering with the dynamic stability of microtubules (*1*−*4*). Microtubules are polymers of tubulin, a 100 kDa α/β heterodimer, which play a pivotal role in the development and maintenance of cell shape in cell division and in cellular signaling and movement. The architecture and the dynamics of the microtubules are central to their varied functions. The microtubules are structurally polar (*5*), with a nongrowing minus end and a growing plus end (*6, 7*). Microtubules exist in a dynamic microequilibrium in the cell milieu in which the stochastic variations in the dynamics and the ability to shorten at one end and grow at the opposite end are fundamental processes in normal cell cycle events. Therefore, agents that bind to tubulin and inhibit microtubule function continue to spark drug discovery efforts. On the basis of the effects of these agents on microtubule stability in cell-free systems, they are classified into two major classes, namely, (i) polymerizing agents such as paclitaxel, discodermolide, epothilones, and eluetherorobins that hypernucleate microtubule assembly and (ii) inhibitors of microtubule assembly such as the vinca alkaloids, cryptophycins, colchicine, and peptides such as hemiasterlin and dolastatin. Hemiasterlin is a naturally occurring marine-derived tripeptide that has been shown to arrest cells in mitosis (*8*). HTI-286, a synthetic analogue of hemiasterlin, has potent antitubulin activity (*9, 10*). The difference between the chemical structures of HTI-286 and hemiasterlin is the presence of a phenyl ring at the N-terminus in the former instead of an indole as shown in Figure 1. HTI-286 inhibits cell proliferation and tubulin polymerization in cell-free assays (*10*). Recent studies at Wyeth have shown that HTI-286 has potent cytotoxicity against KB cells and is active in in vivo tumor models, leading to its recent entry into clinical trials as an antimitotic

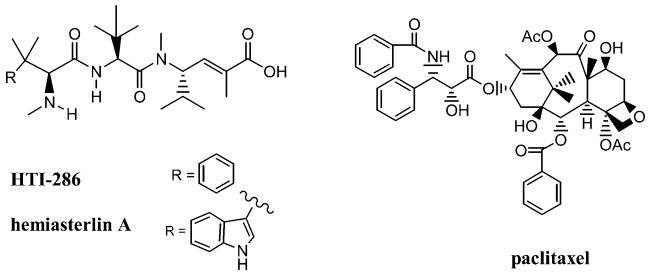

FIGURE 1: Structures of antimicrotubule inhibitors.

* Corresponding author: Tel 845-602-5899; fax 845-602-5687; e-mail. krishng@wyeth.com.
‡ Biophysics/Enzymology, Screening Sciences.
§ Oncology Research.
|| Chemical Sciences.

[1] Abbreviations: MT, microtubules; DRI, differential refractive index; MALS, multiangle light scattering; SEC, size-exclusion chromatography; tubulin monomer, α/β heterodimer.

10.1021/bi035530x CCC: $25.00
Published on Web 11/01/2003

agent (*10*). These biological studies (*11*) have also shown that the cells overexpressing the drug transporters MXR and MRP1 are sensitive to HTI-286. Unlike other antimicrotubule agents such as paclitaxel, docetaxel, vinorelbine, or vinblastine, HTI-286 has substantially lower affinity for multidrug resistance protein (P-glycoprotein). The studies also showed that HTI-286 modified the structure of microtubules in cells at low nanomolar concentrations and induced mitotic arrest and apoptosis.

The above-mentioned findings have prompted our studies to characterize the binding interactions of HTI-286 with tubulin and the effect of such interactions on the stability of tubulin and microtubules (MTs). Moreover, the natural analogue, hemiasterlin A, was previously shown to be a potent antimitotic agent (*8*). As a result of the clinical status of HTI-286 and the antimicrotubule activity of hemiasterlin, there is significant interest in comparing the in vitro effects of these two analogues on tubulin and microtubules. One of the challenges in characterizing the affinity and thermodynamics of tubulin interactions with such agents is the intrinsic ability of tubulin to oligomerize in the presence of inhibitor. Presently, most available binding methods rely on the use of radiolabeled inhibitors. For instance, the interactions of radiolabeled dolastatin 10 (*12*) and radiolabeled crytophycin-52 (*13*) with tubulin were studied by the centrifugal gel-filtration method. This method cannot be used routinely for determining binding affinity of inhibitors within and across chemical series, primarily because of the cost and difficulty of synthesis of radiolabeled materials. Moreover, when such radiolabeled reagents are available, their use is limited to investigation of inhibitors that are competitive and not for those that bind at alternate unique sites. A second method that is frequently used is the method of Timasheff and co-workers, in which the binding affinity to tubulin is determined in a coupled equilibrium of a tubulin polymerization assay (*14*). Their studies have elegantly shown that colchicine binds tubulin heterodimer and the resulting complex inhibits microtubule elongation. Analytical ultracentrifugation methods have been used to deconvolute ligand-induced association of tubulin in the original and seminal work published by Frigon and Timasheff (*15*) and in the very detailed series of studies published by Correia and co-workers (*16*). A similar set of extensive results and analysis is not available for HTI-286, which is a new antitubulin agent. In this work we have developed a combination of biophysical methods to determine the thermodynamics of HTI-286−tubulin interactions.

To determine the thermodynamics of the interactions, we first characterized the oligomeric state of tubulin in the presence of the inhibitor using transport methods such as analytical ultracentrifugation and size-exclusion chromatography coupled to multiangle light scattering analyses. In combination with these transport studies and using isothermal titration calorimetry, we determined the thermodynamics of the interactions of HTI-286 with tubulin for the initial binding step. We have also studied the effects of HTI-286 on preassembled microtubules using fluorescently labeled microtubules to discriminate the effects of HTI-286 from those of taxol. The results of these evaluations demonstrate that (i) HTI-286 oligomerizes tubulin to a discrete 18.5 S species, (ii) the initial binding of HTI-286 to tubulin is rapid compared to the formation of the 18.5 S species, (iii) the initial binding of HTI-286 to tubulin is enthalpically driven, (iv) the formation of the 18.5 S tubulin oligomer does not contribute significantly to the observed enthalpy, and (v) HTI-286 depolymerizes microtubules.

MATERIALS AND METHODS

Materials. Microtubule-associated protein- (MAP-) free bovine brain tubulin and rhodamine-labeled tubulin were obtained as dry powders from Cytoskeleton (Denver, CO). PEM buffer [80 mM PIPES, piperazine-*N*,*N*′-bis(2-ethanesulfonic acid), containing 1 mM EGTA, ethylenebis(oxyethylenenitrilo)tetraacetic acid, and 1 mM magnesium chloride] was obtained from Cytoskeleton. HTI-286 was synthesized by previously reported methods (*17*, *18*) and methods developed at Wyeth (*9*). Hemiasterlin A was generously provided by Dr. Raymond J. Andersen (University of British Columbia, Vancouver, Canada). Stock solutions of HTI-286 and hemiasterlin were prepared as 10 mM stock solutions in 100% dimethyl sulfoxide (DMSO).

Size-Exclusion Chromatography and Multiangle Light Scattering. Size-exclusion chromatography (SEC) coupled to multiangle laser light scattering (MALS) was used to obtain information about the molar mass (*19*) and therefore the aggregation state of tubulin. The online light scattering measurements were performed on Wyatt's DAWN EOS multiangle scattering laser photometer with a 25 mW GaAs (gallium arsenide) laser at 690 nm. The concentration of the tubulin was monitored by either the absorbance (diode-array detector) or a differential refractive index (DRI), Optilab, detector. The MALS method yields molar mass distribution and their moments (number-averaged mass, M_n; weight-averaged mass, M_w; and the *z*-averaged mass, M_z), polydispersity, and the root-mean-square (RMS) radius, r_g. The DNDC software was used to calculate the refractive index (RI) calibration constant. ASTRA software was used to process the light scattering data. Tubulin was chromatographed on a Phenomenox Bio-Sep SEC4000 size-exclusion column or a Shodex OH-pak guard column (rapid light scattering method) with an HP-1090 instrument. The high-performance liquid chromatography (HPLC) solvent, phosphate-buffered saline (PBS), was filtered through an in-line (0.2 μm) filter before entering the column to eliminate dust that might enter the flow cell in the DAWN EOS unit. All HPLC solvents were purged with helium to eliminate potential interference from dissolved air.

The kinetics of tubulin oligomerization in the presence of HTI-286 was determined by the rapid light scattering method. Typically, a fixed concentration of unlabeled tubulin was premixed with substoichiometric or stoichiometric levels of HTI-286 and an aliquot of the complex was applied to the guard column after incubation for 0, 3, and 15 min. Since the analysis time is very short (ca. 2 min), this method is useful in detecting the rate of formation of oligomeric intermediates of tubulin. Elution of tubulin off the column was detected in real time by the UV and DRI concentration detectors.

The full-length sizing column was used to obtain molar mass distribution of tubulin in the absence and presence of the inhibitor. Unlabeled tubulin (2 μM) was preincubated with HTI-286 or hemiasterlin in filtered PEM buffer for 30 min and the resulting solution was chromatographed on the column. The molar mass distribution of tubulin was calculated from the light scattering and concentration detectors.

Analytical Ultracentrifugation. Sedimentation velocity experiments were performed on a Beckman XLI/XLA analytical ultracentrifuge. To investigate the effects of HTI-286 on tubulin, HTI-286 was added to unlabeled tubulin (2 μM) at increasing drug concentrations from 0.5 to 50 μM. The mixture, 400 μL, was loaded into two-channel (1.2 cm path length) carbon-Epon centerpieces in an An-60 Ti rotor. Scans were recorded at 20 °C with a rotor speed of 35 000 rpm, and the signal was detected at 280 nm with a spacing of 0.006 cm in the continuous mode. The sedimentation profiles were analyzed to obtain the distributions of the sedimentation coefficients by use of the program Sedfit (*20*).

To determine the molar mass of tubulin in the presence of HTI-286, a 200-μL sample solution containing 2 μM tubulin and 5 μM HTI-286 was loaded into two-channel (1.2 cm path length) carbon-Epon centerpieces in an An-60 Ti titanium rotor. Sedimentation equilibrium experiments were performed on a Beckman XLI/XLA analytical ultracentrifuge at 20 °C with a rotor speed of 2000 rpm. Scans were recorded at 280 nm with a 0.001 cm spacing, and equilibrium was judged to be achieved when there was no deviation between successive scans taken 6 h apart. The weight-average molar mass of the tubulin aggregate was determined by fitting the equilibrium profile into the following equation with the Origin software, version 3.78:

$$C_r = C_0 \exp[M(1 - \bar{\nu}\rho)\omega^2(r^2 - r_0^2)/2RT] + \text{base}$$

where C_r is absorbance at radius r; C_0 is absorbance at reference radius r_0; M is the molar mass of the macromolecule; $\bar{\nu}$ is the partial specific volume of the macromolecule (in milliliters per gram); ρ is the density of the solvent; ω is the angular velocity of the rotor; R is the gas constant; T is temperature; and base is baseline offset. The partial specific volume of tubulin (0.7264 g/cm^3) used in the fitting was obtained from the amino acid sequence of porcine brain tubulin by use of the Sednterp program (*21*).

Isothermal Titration Calorimetry. The thermodynamics of the interactions of HTI-286 with tubulin were determined by use of a Microcal VP-ITC isothermal titration calorimeter. Two kinds of calorimetric titration experiments were performed; the rationale and design of the experiments are described below.

(*i*) *Serial Titration Experiment*. The purpose of this experiment is to determine the thermodynamic parameters including the enthalpy and binding affinity of the interactions of HTI-286 with tubulin at various tubulin concentrations. In this experiment, HTI-286 was sequentially titrated into tubulin with a standard equilibration time of 5 min between injections and duration of 2 s/μL for each injection. The serial titration experiment was performed at tubulin concentrations of 1, 2, 5, 10, and 13 μM. For instance, 70 μM HTI-286 solution was titrated into 2 μM tubulin with 17 × 6 μL injections and a stirring speed of 300 rpm. All binding experiments were carried out at 25 °C. Data were analyzed with Microcal Origin software, by fitting to a single-site binding model.

(*ii*) *Batch Titrations*. The purpose of the batch experiment is to deconvolute the heats associated with the binding from the tubulin oligomerization events. The batch experiments were conducted with four successive injections of inhibitor at a constant spacing of 30 min between injections, to determine the initial heat of binding and the heat of oligomerization following the binding step. This is in contrast to the serial ITC experiment that measures the total heat of the reaction due to 17−35 successive titrations of the ligand into protein at a constant spacing of 5 min between injections. Four successive aliquots of HTI-286 with injection volumes of 2, 6, 45, and 45 μL were titrated into 2 μM tubulin with a delay time of 10 min after the first injection and 30 min between each successive injection. This experiment was also performed at tubulin concentrations of 3 and 4 μM. The duration of the injection was kept constant at 2 s/μL. The stock solution of HTI-286 was prepared in PEM buffer at 70 μM and titrated into the tubulin solution in the cell. In the control experiment, the HTI-286 stock solution was titrated into PEM buffer in the cell, and the above-mentioned injection sequence was used to obtain the heat of dilution. The area under each of the four injection peaks was integrated and the heat of dilution was subtracted from the actual heats by use of the Origin software.

Fluorescence Binding Assays. Fluorescence spectroscopic methods were used to determine the binding potency of HTI-286 and hemiasterlin A to tubulin. Either the fluorescently labeled or unlabeled tubulin was used in the binding assays. Bovine brain tubulin consists of eight tryptophan residues that emit fluorescence at a maximum wavelength of 335 nm due to excitation at 295 nm. The changes in the quantum yield and emission maximum of the tryptophan residues are good probes for determining binding affinity and to detect conformational changes that can occur in the presence of inhibitors. In the case of the labeled tubulin, changes in the quantum yield of the extrinsic fluorescence probe, rhodamine, in the presence of HTI-286 and hemiasterlin A were used to determine the binding affinity and stoichiometry to tubulin. Rhodamine-labeled tubulin has maximum fluorescence at 580 nm due to excitation at 560 nm. The intrinsic fluorescence emission of tryptophan or the extrinsic fluorescence of rhodamine in the absence and presence of increasing concentrations of the inhibitors was monitored on a Jobin-Yvon Horiba fluorometer (Fluoromax-2). The excitation and emission scans were acquired with monochromator bandwidths of 1 and 3 nm, respectively. The tubulin fluorescence spectra were scanned in the ratio mode (S/R, signal/reference) to compensate for variations in lamp output as a function of wavelength.

The tubulin−inhibitor binding experiments were run in the following format. The rhodamine-labeled tubulin was freshly dissolved in PEM buffer at a final concentration of 5 mg/mL. The tubulin stock solutions were diluted to 2 μM (unlabeled tubulin) or 0.5 μM (rhodamine-labeled tubulin) in PEM buffer, respectively, and then aliquoted into nine quartz cuvettes. Alternatively, unlabeled and labeled tubulin was combined at equimolar concentrations to a final concentration of 4 μM and aliquoted as described above. The inhibitors were prepared by serially diluting the master stock 50-fold to the desired inhibitor concentration (1×) in each cuvette. The initial fluorescence of the rhodamine-labeled tubulin was measured. HTI-286 or hemiasterlin was then titrated into the tubulin in the cuvettes at concentrations ranging from 0 to 20 μM. The fluorescence intensity of the tubulin in the absence and presence of the inhibitors was measured after preincubation for 10 min. The fluorescence changes were fitted to a quadratic equation (*22*) to obtain

apparent dissociation constants of tubulin−inhibitor interactions.

Tubulin Polymerization and Depolymerization Assay. The kinetics of formation of microtubules were quantified by the UV-based assay. Microtubules were prepared in the presence of glycerol and formation of these polymers was monitored in real time due to the increase in UV absorption at 340 nm. After formation of the stable microtubule structures, HTI-286 was added and the decrease in UV absorption due to depolymerization was continuously monitored at 340 nm. Glycerol-induced microtubules were prepared by adding 220 μL of G-PEM buffer [80 mM PIPES, pH 6.9, 0.5 mM $MgCl_2$, 1 mM EGTA, and 1 mM guanosine triphosphate (GTP)] containing 10% glycerol into 1 mg of bovine brain tubulin to produce microtubules at a final concentration of 4.5 mg/mL. The tubulin solution was incubated at 35 °C for 30 min and the UV absorption at 340 nm was continuously monitored at 2-min time intervals. The UV absorbance reached a steady-state value at 30 min, after which varying amounts of HTI-286 were added to determine the stability on the basis of the decrease in UV absorbance.

Depolymerizing Effects of HTI-286 on Microtubules by the Fluorescence Microscopy Method. For this assay, microtubules were prepared from rhodamine-labeled tubulin to visualize the morphology of the structures in a fluorescence microscope in the absence and presence of inhibitors. The tubulin was polymerized in glycerol by combining 1.5 mg/mL labeled tubulin with unlabeled tubulin to a final concentration of 5.0 mg/mL. The mixture of labeled and unlabeled tubulin was polymerized in G-PEM buffer containing 10% glycerol at 35 °C. An aliquot of the polymerized tubulin solution (5 μL) was placed on a glass slide and covered with a coverslip prior to imaging of the sample in a Nikon Eclipse TE200 microscope equipped with a Spot Digital camera. HTI-286 was combined with microtubules and incubated at either 35 °C or ambient temperature for specified times prior to detection by imaging via microscopy.

RESULTS

HTI-286 Oligomerizes Tubulin to a Discrete Ring Structure. The oligomerization state of tubulin in the absence and presence of HTI-286 or hemiasterlin was determined by analytical ultracentrifugation and SEC/MALS methods. Analytical ultracentrifugation methods have been used previously to study tubulin association in the presence of various small molecules (*23*−*25*) and are therefore an important solution-based method to determine the effects of HTI-286. Figure 2 shows the distribution of sedimentation coefficients of tubulin as a function of HTI-286 concentration. Monomeric tubulin is a α/β heterodimer that migrates with a sedimentation coefficient of ca. 5.3 S. When 0.5 or 1.0 μM HTI-286 was added to tubulin monomer (2 μM), additional peaks with higher sedimentation coefficients appear, consistent with the formation of larger tubulin oligomers. In the presence of 1 molar equiv of HTI-286, tubulin forms a major species corresponding to a sedimentation coefficient of ∼18.5 S with 10 and 15 S species as minor components. Further addition of HTI-286 does not increase the size of the oligomers beyond the 18.5 S species. The oligomerized tubulin is stable as a function of time, at least for a few days. The 18.5 S tubulin species is consistent with the formation

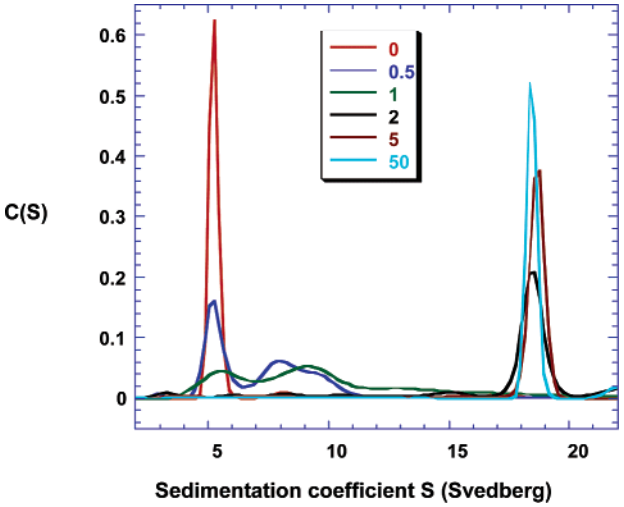

FIGURE 2: Sedimentation coefficient distribution, *C*(S), plots at increasing HTI-286 concentrations. Sedimentation velocity experiments were performed as described under Materials and Methods with 2 μM tubulin and HTI-286 concentrations of 0 μM (red), 0.5 μM (dark blue), 1 μM (green), 2 μM (black), 5 μM (brown), and 50 μM (cyan).

of a ring structure as shown previously for complexes formed with cryptophycin (*25*).

An estimate of the binding stoichiometry of HTI-286 per tubulin monomer was investigated with an N-terminally modified stilbene analogue of HTI-286 by the analytical ultracentrifugation method. In this experiment, tubulin at 10 μM was combined with a saturating concentration of the stilbene analogue and the comigration of the inhibitor with tubulin was monitored at the unique absorption wavelength of the inhibitor, 312 nm. The concentration of the stilbene analogue that comigrated with the 18.5 S tubulin oligomer corresponded to a binding stoichiometry of one inhibitor per tubulin. The formation of the oligomer appears to be ligand-induced.

Since the oligomers obtained at the stoichiometric ratio of tubulin to HTI-286 are stable in solution, a sedimentation equilibrium experiment was set up to estimate the molar mass of tubulin in complex with HTI-286. For this centrifugation experiment a sample containing 2 μM tubulin and 5 μM HTI-286 was prepared. The equilibrium profile (Figure 3) was analyzed with Origin software by fitting to a single ideal species model to obtain the weight-average molar mass. The weight-average molar mass is ca. 1300 kDa.

In addition to analytical ultracentrifugation, size-exclusion chromatography (SEC) was used to obtain the molar mass of tubulin in the absence and presence of inhibitors. SEC offers speed of analyses of tubulin samples and the method has been used previously to determine the aggregation state of tubulin in the presence of antitubulin agents including vinca alkaloids (*26*) and hemiasterlin (*27*). For instance, Hamel and co-workers (*27*) showed that tubulin oligomerizes in the presence of hemiasterlin with stable small oligomers forming at substoichiometric concentrations of the inhibitor and larger end-stage oligomers forming in the presence of molar equivalents of the inhibitor. However, the application of SEC methodology is limited when the nascent tubulin oligomers are unstable during the chromatographic separation. To resolve this issue, we coupled the chromatography method with the multiangle laser light scattering method to

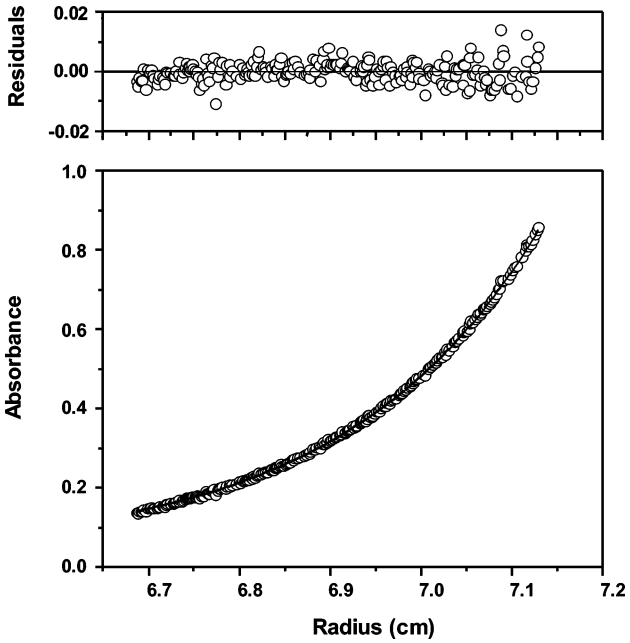

FIGURE 3: Sedimentation equilibrium analyses of the tubulin oligomers formed during the incubation of 2 μM tubulin with 5 μM HTI-286. The lower panel corresponds to the absorbance signal at 280 nm after equilibrium has been established at 2000 rpm, and the solid line corresponds to the curve fit to a single ideal species. The upper panel corresponds to the residuals of the curve fit in the lower panel.

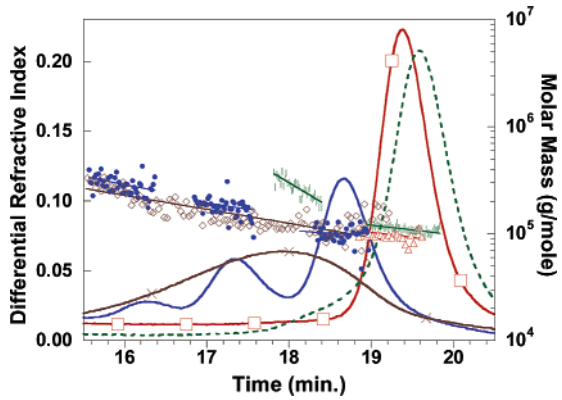

FIGURE 4: Chromatograms and molar mass distributions of tubulin in the absence and presence of inhibitors. Tubulin (2 μM) was preincubated for 30 min with either hemiasterlin A or HTI-286 in PEM buffer. The samples were chromatographed on a Bio-Sep SEC4000 column in PBS buffer and the elution was monitored by use of multiangle light scattering and DRI concentration detectors as described under Materials and Methods. The DRI chromatograms (on the left *y*-axis) of tubulin in the absence (□, red solid curve) and in the presence of 0.5 μM hemiasterlin A (blue solid curve), 0.5 μM HTI-286 (green dashed curve), or 20 μM HTI-286 (×, black solid curve) show the elution of the different tubulin aggregates over time. The corresponding molar masses (on the right *y*-axis) of the tubulin aggregates in each elution peak are graphed as follows: tubulin in the absence (△, red) and in the presence of 0.5 μM hemiasterlin A (●, blue), 0.5 μM HTI-286 (|, green), or 20 μM HTI-286 (◇, black).

obtain the solution molar mass of tubulin in the absence and presence of HTI-286 or hemiasterlin A in real time. Combining the SEC and MALS methods therefore allows for the rapid estimation of molar mass and identification of unstable and stable oligomers. Moreover, by coupling light scattering to chromatography, the association state of tubulin can be obtained in a short guard column without the need for separation.

Tubulin (2 μM) was incubated with 0.5 or 20 μM HTI-286 or 0.5 μM hemiasterlin A for 30 min prior to chromatography on the size-exclusion column. The resulting DRI chromatogram of tubulin and the weight-averaged molar mass of the elution peaks are shown in Figure 4. The tubulin peak eluting with a retention time of about 19.5 min corresponds to the tubulin monomer (100 kDa), based on molar mass calculation with the Debye formalism (ASTRA software). The monomer molar mass is consistent with the molar mass estimated from the sequence of the α/β chains of tubulin. Substoichiometric concentrations of hemiasterlin A induced the formation of multiple intermediates of tubulin oligomers corresponding to dimer of average molar mass of 220 kDa (17.3 min) and trimer of 330 kDa (16.2 min). In the presence of hemiasterlin, the tubulin monomer has a shorter retention time (18.5 min), possibly due to changes in the shape of the inhibitor-complexed tubulin that is in equilibrium with free tubulin. Saturating concentrations of hemiasterlin A (for instance, 20 μM) induce the formation of stable tubulin oligomers correponding to a molar mass of 1100 kDa.

Contrary to the results observed for hemiasterlin, the HTI-286/tubulin complex migrates as a broad peak in which the trailing edge overlaps with the elution peak of the uncomplexed tubulin. Furthermore, HTI-286 does not induce the formation of stable oligomers of tubulin at sub- or superstoichiometric concentrations under identical chromatographic conditions. The average molar mass of tubulin within the broad elution peak is 122 kDa (at stoichiometric excess of inhibitor), which corresponds to a weight-averaged molar mass of tubulin in the monomeric and dimeric state (Figure 4). In the presence of 0.5 μM HTI-286, the major peak corresponds to the monomeric form of tubulin (19.6 min) with a slight shoulder around 18.5 min due to the instability of the oligomers. When the complex of tubulin with HTI-286 was chromatographed on a guard column instead of a sizing column, the tubulin peak migrated as a sharp peak. The estimated molar mass of tubulin oligomers from the guard column is 1100 kDa, corresponding to a structure consisting of approximately 11 monomer units, which is comparable in size to the discrete 18.5 S ring structure from the ultracentrifugation studies. The molar mass estimates of the ring structure of about 1100 kDa by light scattering and 1300 kDa in sedimentation equilibrium are within 17% with respect to the mean value of 1200 kDa. The dissociation of tubulin is minimized during chromatography on the guard column because the residence time of tubulin is greatly reduced compared to a sizing column, thereby producing sharp elution peaks. Moreover, when the sizing column was preequilibrated with running buffer containing HTI-286, the tubulin elutes as a sharp peak with no broadening effects (data not shown). Therefore, the broad elution peak in the sizing column is due to kinetic instability, resulting in the dissociation of the tubulin/HTI-286 complex on the column due to faster off-rates. Thus, tubulin oligomerizes to a discrete size in the presence of both HTI-286 and hemiasterlin, although the complexes formed by the latter are more stable than with HTI-286.

Tubulin 18.5 S Species Forms Slowly. The kinetics of oligomerization of tubulin was monitored by the rapid light scattering method. In this method, the conversion of the

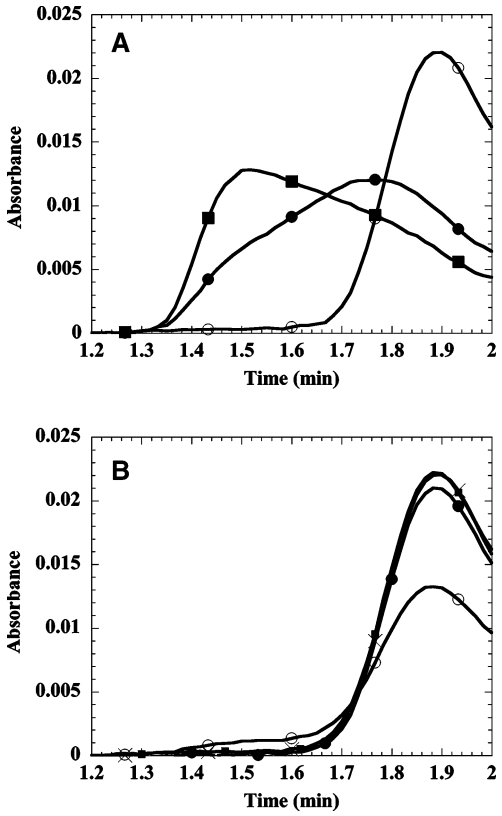

FIGURE 5: Kinetics of formation of tubulin oligomers. (A) Chromatograms of tubulin in the absence and presence of equimolar concentrations of HTI-286 in the guard column. Tubulin (2 μM) was combined with PEM buffer alone (○) or with HTI-286 and preincubated for 3 min (●) and 30 min (■) prior to chromatography on the guard column. Tubulin elution was monitored at 280 nm. (B) Chromatograms of tubulin in the absence and presence of equimolar concentrations of HTI-286 in the guard column. Tubulin (2 μM) was combined with PEM buffer alone (×) or with 0.1 μM HTI-286 for 3 min (●) and 20 min (■). To increase the ratio of HTI-286 to tubulin, the concentrations were changed to 0.2 and 1 μM, respectively, and the mixture was incubated for 20 min (○) prior to chromatography.

monomeric tubulin to higher-order oligomers can be evaluated rapidly, because tubulin elution occurs within 2 min on the guard column. Figure 5A shows the time-dependent formation of tubulin oligomers in the presence of equimolar concentrations of HTI-286 and tubulin. This concentration ratio was chosen because the analytical ultracentrifugation analyses show that tubulin forms one major species (18.5 S) under equilibrium conditions. The kinetics of formation of tubulin oligomers in Figure 5A suggest that HTI-286 rapidly induces the formation of intermediate tubulin oligomers within 5 min (retention time of about 1.75 min). The size distribution of tubulin shifts from the intermediate oligomeric species to the 1100-kDa species (retention time of 1.5 min) upon preincubation of HTI-286 with tubulin for 30 min. In both instances the shift to the higher molar mass is accompanied by a decrease in the tubulin monomer peak at 1.9 min. Thus, the 18.5 S tubulin oligomer forms slowly after preincubation for 30 min.

In the presence of 0.1 μM HTI-286, corresponding to a tubulin/HTI-286 ratio of 20 (Figure 5B), there is no significant increase in the molar mass of tubulin after 3 and 20 min of incubation. However, when the tubulin/HTI-286 ratio was decreased from 20 to 5, the formation of tubulin oligomers is evident (Figure 5B) in the broad elution profile of tubulin, ranging from retention times of 1.4 and 1.7 min. Thus, the formation of tubulin oligomers is dependent on both the concentration of HTI-286 and the time of incubation.

HTI-286 Interactions with Tubulin Are Enthalpically Driven. In light of the observation that HTI-286 induced the oligomerization of tubulin, the thermodynamics of the interactions of HTI-286 with tubulin was investigated by isothermal titration calorimetry. Particularly, the observations that the tubulin oligomers form slowly and the rate depends on the concentration of HTI-286 relative to tubulin are important for setting up ITC experiments. These observations in conjunction with the ITC results were used to deconvolute the thermodynamics of the binding from the oligomerization event. The ITC experiments were designed to monitor the heat of tubulin oligomerization, using the 30-min spaced injection sequence in the batch experiments, as described under Materials and Methods. Since the multiangle light scattering experiments described above demonstrate that tubulin does not oligomerize at low molar ratios of HTI-286/tubulin, the corresponding 6 μL injection in the ITC experiment should yield heat associated primarily with the binding step. Similarly, the heat associated with the binding and oligomerization steps should be measurable for the 45 μL injection (high molar ratio of HTI-286/tubulin) for the duration of the injection and in the subsequent equilibration step.

The raw ITC results in Figure 6A show that the interactions of HTI-286 with tubulin are associated with release of heat. Heat is evolved during the duration of the injection, consistent with rapid binding of HTI-286 to tubulin. The heat evolved increases with increase in the bound density of HTI-286. However, there is no evidence for absorption or release of heat beyond the single injection sequence for either the low or high molar ratios of tubulin to HTI-286. Since the oligomers form slowly, the ITC results suggest that the heat evolved is primarily associated with the binding of HTI-286 to tubulin monomer.

To evaluate the correlation between the heat evolved and the bound density of HTI-286, batch experiments were carried out with 3 μM tubulin. Additionally, the heat of binding was also measured in a serial ITC titration experiment, in the presence of tubulin at 10 μM, to compare with the results of the batch experiments at the lower tubulin concentration. The rationale and the analyses of the results are as follows. In the ITC experiment the heat evolved can be represented by

$$Q_i = V\Delta H_{obs}\Delta L_i \quad (1)$$

where V is the volume of the cell, ΔH_{obs} is the enthalpy of the binding per mole of ligand, and ΔL_i is the increase in the concentration of the bound ligand after the ith injection. For a simple single-site binding model, eq 1 can be expressed as

$$Q_i/P_t = V\Delta H_{obs}K_a[L] \quad (2)$$

The ratio Q_i/P_t is the normalized heat evolved for a given free ligand concentration of L, and P_t is the total tubulin concentration. According to eqs 1 and 2, the normalized heat is proportional to the bound density for a single-site model. Equation 2 is not valid when the observed enthalpy is a sum

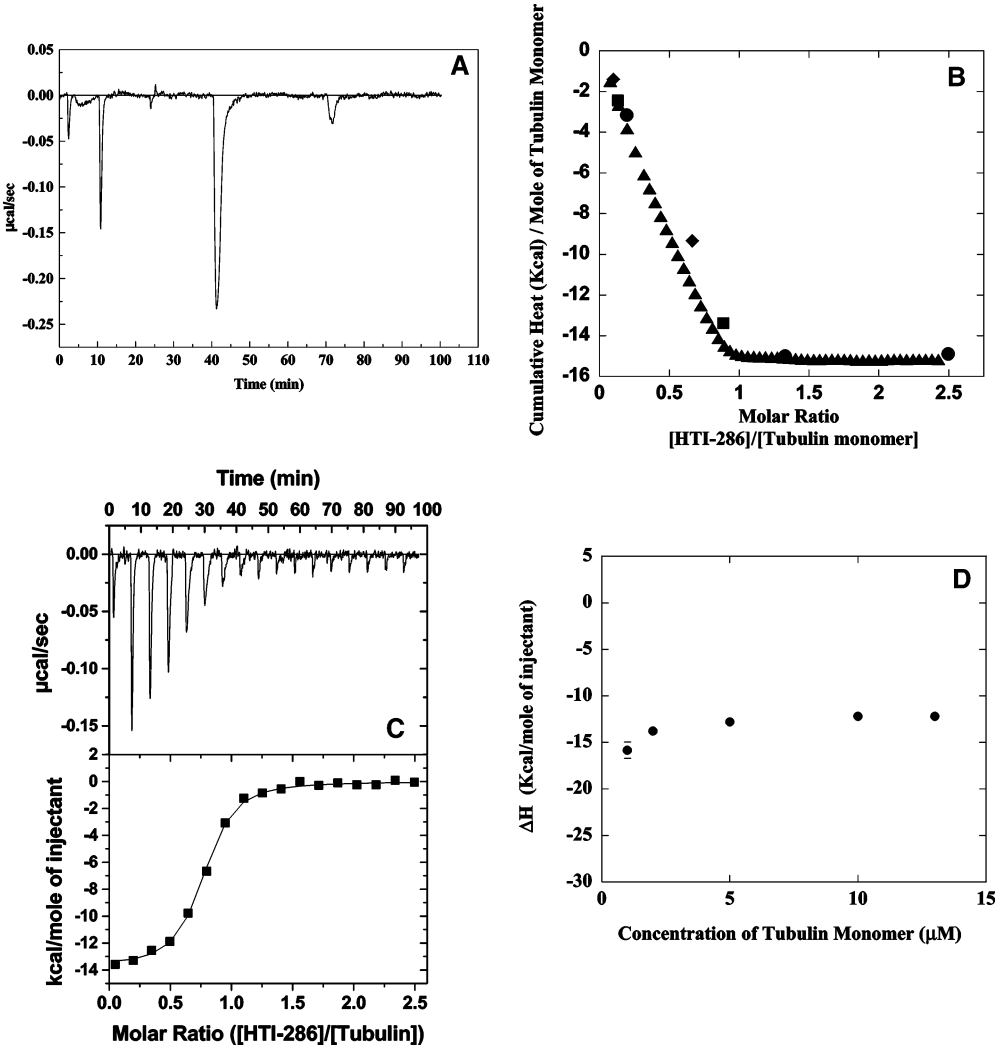

FIGURE 6: Calorimetric titration of HTI-286 with tubulin in PEM buffer at 25 °C. (A) Batch titration of tubulin monomer (2 μM) with 70 μM HTI-286 in the syringe, in PEM buffer. The raw ITC data are shown as power versus time after baseline subtraction. The injection volumes correspond to 2, 6, 45, and 45 μL of the HTI-286 solution. The durations of the injection are 4, 12, 90, and 90 s, respectively. (B) Comparison of the cumulative heats from the batch and serial titration of tubulin with HTI-286. Tubulin monomer, 2 μM (●), 3 μM (■), or 4 μM (◆), was titrated with 70 μM HTI-286 in the syringe according to the injection sequence described for panel A. Tubulin (10 μM, ▲) was sequentially titrated with 140 μM HTI-286 in the syringe. In each of the batch and the serial titration experiments, the baseline was subtracted from the raw power and then the area under the peaks was obtained by integration. The cumulative sum of the area under the peaks was obtained for each of the titrations. The cumulative heats were then divided by the respective tubulin concentration to obtain the normalized area for each of the injections. (C) Serial titration analyses of the interaction of tubulin with HTI-286. Tubulin monomer (2 μM) with 70 μM HTI-286 in the syringe, in PEM buffer. The upper panel shows raw data in power versus time after baseline subtraction. The area under each injection peak is proportional to the heat produced. The lower panel shows the binding isotherm created by plotting the integrated peaks against the molar ratio of HTI-286 added to tubulin dimer. Nonlinear regression analysis was done in terms of a single-site binding model. The theoretical curves fitted to the integrated data yield $\Delta G = -10.7$ kcal/mol and $\Delta H = -13.77$ kcal/mol. (D) Effect of tubulin concentration on the observed enthalpy. Tubulin at various concentrations was titrated with HTI-286 as described under Materials and Methods. Data were analyzed according to the single-site model by nonlinear regression analysis for each of the data sets. The theoretical curves fitted to the integrated data were used to estimate ΔH_{obs} for each tubulin concentration.

of the binding and oligomerization steps and when both steps contribute significantly to the overall enthalpy. Therefore, if the heat of oligomer formation is of significant magnitude or if the binding does not fit a single binding site model, then the normalized heats will vary depending on tubulin concentration. In Figure 6B the normalized heats from the batch experiments conducted at 2, 3, and 4 μM tubulin are compared with the normalized heats evolved for the standard serial titration at 10 μM tubulin. The normalized heats measured at low molar ratios of HTI-286 to tubulin in the batch and serial titration experiments are nearly identical. This result is consistent with the observations from the light scattering analyses that tubulin oligomers do not form rapidly during the short duration of the injection step (12 s, 6 μL injection). However, at high molar ratios of HTI-286 to tubulin, the binding and oligomer formation should occur concurrently for the 45 μL injection within the duration of the injection (90 s). The results in Figure 6B show that the cumulative values of the normalized heats are identical in the batch (2, 3, and 4 μM tubulin) and the serial titration experiments. Therefore, the normalized heat evolved is a function of the bound density of HTI-286 and it appears to be independent of the tubulin concentration or the equilibration time. Thus, the experiments confirm the previous observation that the heat associated with the tubulin oligomerization and specifically the ring formation step is negligible compared to the exothermic heats due to the initial binding event.

Further, the thermodynamics of HTI-286 interactions with tubulin were investigated by the serial titration ITC method, at various concentrations of tubulin. Figure 6C shows that the association of HTI-286 with tubulin is enthalpically driven with an apparent ΔH of -13.8 kcal/mol and a $T\Delta S$ value of -3.74 kcal/mol. The estimated enthalpy increases slightly at the lowest tubulin concentration, although within the limits of experimental error the enthalpy values are independent of the tubulin concentration (Figure 6D). The K_D value of tubulin−HTI-286 interactions is approximately 94 nM (1 μM tubulin) and 90 nM at 13 μM tubulin. The stoichiometry is consistent with one HTI-286 bound per tubulin monomer. As stated above, the enthalpy associated with the tubulin oligomerization step is negligible compared to the observed net enthalpy. The combined ITC results described here, therefore, demonstrate that the observed enthalpy is associated with the interactions of HTI-286 with tubulin and not the tubulin ring formation event.

HTI-286 Binding to Tubulin Induces Spectral Changes in Tubulin. Fluorescence spectroscopy was used to determine the binding affinity of HTI-286 analogues because this is a practical alternative for determining binding affinity of antitubulin agents due to the inherent ease and speed of the experiments. Since the fluorescence method has been used to determine the binding affinity of other antitubulin agents, it is important to determine the affinity of HTI-286 and hemiasterlin to tubulin by this technique, for comparison purposes. In this work the changes in the fluorescence of tryptophan residues or the extrinsic probe rhodamine were used to estimate the apparent binding affinity. The fluorescently labeled bovine brain tubulin is singly labeled with rhodamine at the lysine residues on the heterodimeric protein. Rhodamine-labeled tubulin emits maximally at 580 nm due to excitation of the fluorescent probe at 560 nm. The fluorescence quantum yield of the labeled tubulin is successively quenched upon binding to increasing concentrations of HTI-286 (Figure 7A). The changes in the fluorescence intensity of rhodamine-labeled tubulin at 580 nm were used to estimate the apparent dissociation constant of HTI-286 by the use of a quadratic equation (*22*). The binding affinity of HTI-286 to rhodamine-labeled tubulin is 260 nM. Figure 7B shows the binding isotherm of HTI-286 in the presence of 0.5 μM tubulin. Hemiasterlin A similarly quenched the fluorescence of rhodamine-labeled tubulin and the resulting binding affinity is 180 nM, comparable to that of HTI-286 (data not shown). Both HTI-286 and hemiasterlin A bind tubulin saturably. The K_D was also determined at a higher tubulin concentration of 4 μM. Since rhodamine has a high fluorescence quantum yield, for the binding experiment at high tubulin concentration, 2 μM labeled tubulin was combined with 2 μM unlabeled tubulin. In the presence of 4 μM tubulin the binding affinity is 440 nM, a value that is slightly higher than the affinity estimated at the lower concentration. There is no evidence for time-dependent binding of HTI-286 at 4 μM tubulin. Because the tubulin is modified by the rhodamine fluorophore and the modification is an average of 1 fluorophore/tubulin, any one of the surface-accessible lysine residues could be modified. As a result, in certain instances, at the low tubulin concentrations (0.5 μM) we have observed time-dependent effects on binding. This effect is presumably due to fluorescence changes during tubulin association, depending on the position of the modified lysine residue.

Further, the interactions of HTI-286 with unlabeled tubulin were also evaluated from the changes in the tryptophan fluorescence of tubulin. In the presence of HTI-286, the fluorescence emission maximum of tryptophan residues is blue-shifted by about 4 nm (Figure 7C). The blue shift in the fluorescence of the tryptophan residues is indicative of a conformational change resulting in a more hydrophobic environment of these residues. The fluorescence intensity decrease at 332 nm in the presence of increasing concentrations of HTI-286 was used to estimate the binding affinity. The apparent K_D is ca. 100 nM. Since the quenching of tryptophan fluorescence is not large in comparison to the changes in rhodamine fluorescence, the change in the emission maximum of the fluorescence was also used to estimate the affinity. The binding affinity determined by the wavelength-shift method, 100 nM, is nearly identical to the affinity determined by the intensity method. Figure 7D shows the binding isotherm of HTI-286 from the tryptophan fluorescence method. Thus, the K_D values determined in the fluorescence experiments are comparable within the limits of experimental error. Since the dissociation constant is consistent with the ITC results, it follows that the binding affinity is due to the initial binding step and is not associated with the ring formation event. HTI-286 also altered the circular dichroic absorption spectrum of tubulin in the far UV, consistent with the conformational changes observed via the fluorescence method (Figure 7E). The changes in the circular dichroic (CD) and fluorescence spectra of tubulin appeared to occur within 10 min after the addition of the inhibitor. In summary, the binding affinities of HTI-286 to tubulin obtained from the fluorescence methods are comparable, although the affinity by the rhodamine method is always slightly lower.

HTI-286 Promotes Depolymerization of Microtubules. The effect of HTI-286 on microtubules was investigated by a UV-based continuous assay and the morphology of the tubulin structures in the absence and presence of inhibitors was visualized by a fluorescence microscopy assay, as described under Materials and Methods.

The time course of polymerization was monitored by the changes in UV absorbance at 340 nm (due to light scattering by polymers) as shown in Figure 8. At 30 min, the UV absorbance reached a plateau due to the formation of microtubules. When increasing concentrations of HTI-286 were added, the UV absorbance at 340 nm decreased progressively due to depolymerization of microtubules. The rate and extent of depolymerization depends on the amount of HTI-286 added. At a molar ratio of 0.25 of HTI-286/tubulin dimer, the UV absorbance decreased slowly and only a slight absorbance change was observed. In contrast, when the ratio was increased to 0.5 and beyond, the UV absorbance dropped rapidly and approached the background reading.

Tubulin polymers grown in the presence of glycerol are large, with an average length significantly exceeding 10 μm, and therefore can be readily visualized under a microscope (Figure 9A). Paclitaxel binds and stabilizes microtubules as evidenced by resistance to cold-induced depolymerization (see Figure 9B). In contrast, when the microtubules were incubated with HTI-286, they progressively depolymerized as a function of time. As shown in Figure 8C, when an

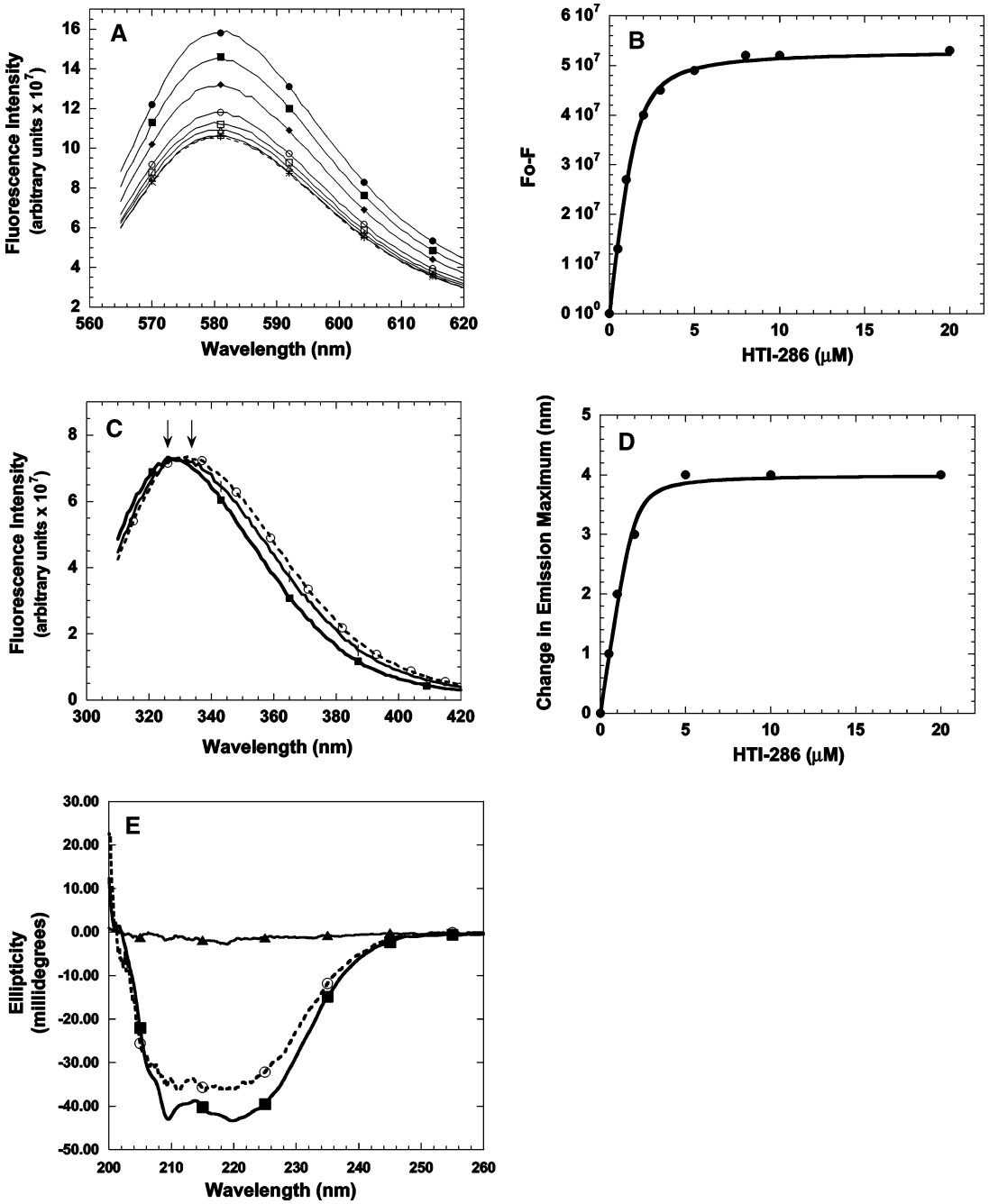

FIGURE 7: Change in fluorescence and CD absorption of tubulin in the presence of HTI-286. (A) Fluorescence spectra of rhodamine-labeled tubulin. Tubulin was preincubated with buffer (●) or with HTI-286 at 0.5 μM (■), 1 μM (◆), 2 μM (○), 3 μM (□), 5 μM (△), 8 μM (×), 10 μM (|), and 20 μM (---) for 10 min prior to obtaining fluorescence spectra (excitation wavelength is 560 nm). (B) Binding isotherm of the interactions of tubulin with HTI-286. Labeled tubulin (0.5 μM) was incubated with 0−20 μM HTI-286 for 10 min (●). The change in the fluorescence of rhodamine at 580 nm, $F_0 - F$, in the presence of increasing concentrations of HTI-286 is proportional to the bound inhibitor concentration. The solid line corresponds to the curve fit to the quadratic equation. (C) Fluorescence spectra of unlabeled tubulin (2 μM) in the absence (○) and presence of HTI-286 at 1 μM (|) or 20 μM (■). Arrows indicate the emission maximum of tubulin in the absence (332 nm) and presence (324 nm) of HTI-286. (D) Binding isotherm of HTI-286 derived from changes in the emission maximum of the fluorescence of tryptophan residues in unlabeled tubulin. Tubulin (2 μM) was incubated with 0−20 μM HTI-286 for 10 min (●). The change in the emission maximum (see panel C) with increasing concentrations of HTI-286 was fit to a quadratic equation (solid line). (E) Far-UV CD spectra of tubulin (2 μM) in the absence (○) and presence (■) of 4 μM HTI-286. HTI-286 alone has negligible CD absorption (▲).

aliquot of HTI-286 was added to microtubules and then the sample was viewed under the microscope immediately afterward (at ambient temperature), the depolymerizing effects of HTI-286 are evident at 5 min (Figure 9C, panel A) as the microtubules begin to lose the filamentous structure. Upon incubation of microtubules with HTI-286 for 10 min at 37 °C (panel B) the microtubular structure completely disappears, consistent with the UV kinetic data shown in Figure 8. Both the UV and fluorescence microscopy methods are, however, insensitive to the detection of small aggregates due to physical limitations of the methods (*28*). To determine the average molar mass of depolymerized microtubule, the MALS method was used in conjunction with a guard column. The preformed complex of microtubules with HTI-286 (equimolar amounts) was preincubated for approximately 2 and 4 h, and the resulting mixture was chromatographed on

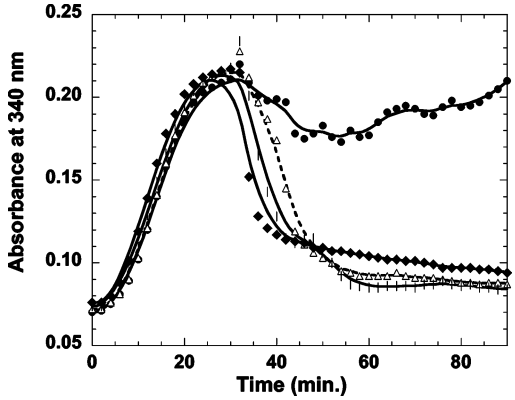

FIGURE 8: Time course of tubulin polymerization induced by glycerol and depolymerization induced by HTI-286. Microtubules (45 μM) were prepared for polymerization in glycerol-containing buffer as described under Materials and Methods. The increase in the absorbance signal at 340 nm was continuously monitored as a function of time up to 30 min. After 30 min, HTI-286 was added to the microtubules at various concentrations corresponding to inhibitor:tubulin dimer ratios of 0.25 (●), 0.5 (△), 1 (|), and 5 (◆).

a guard column to determine tubulin size. MALS analyses of the depolymerized tubulin by the guard column method showed that HTI-286 induced the formation of tubulin oligomers, the 11-mer, as the major component (data not shown). The microtubules depolymerize slowly such that the oligomeric structures of tubulin do not appear after shorter incubation times.

DISCUSSION

HTI-286 Binding to Monomeric Tubulin. Antitubulin agents such as the vinca alkaloids and other peptide-like agents inhibit tubulin function in different ways, depending on the intracellular concentrations of the inhibitor. In the first mode, in the presence of high concentrations of inhibitor, microtubules are depolymerized, thereby preventing MT function in the cell. The second mode of action is due to the alteration of tubulin dynamics due to inhibitor binding to the ends of the MTs or to the addition of inhibitor−tubulin complex to these ends. The third binding mode is direct interaction with soluble tubulin to form ring structures such that the MT dynamics are altered due to a lowering of the equilibrium pool of soluble tubulin. The central question in the mode of action studies is the affinity of the inhibitors to tubulin monomer and the effect of the binding on the oligomerization state of tubulin. Previous studies on the formation of tubulin oligomers in the presence of inhibitors were typically conducted under equilibrium conditions. Therefore, the thermodynamics of inhibitor binding to tubulin was linked to tubulin oligomerization. Remarkably, we found that the tubulin oligomers, including the 18.5 S species, form slowly in the presence of HTI-286 in the kinetic studies by the light scattering method. The ITC results, however, show that the initial binding is fast and occurs in the duration of the injection. This observation enabled us to deconvolute the binding affinity of the interactions of tubulin monomer with HTI-286 from the linked-tubulin association step in the ITC studies. The thermodynamics of HTI-286 interactions with tubulin is accompanied by a negative enthalpy change of about 14 kcal/mol (at 25 °C) and the observed enthalpy does not vary significantly with tubulin concentration. In considering other ITC studies, for instance, the dimerization of

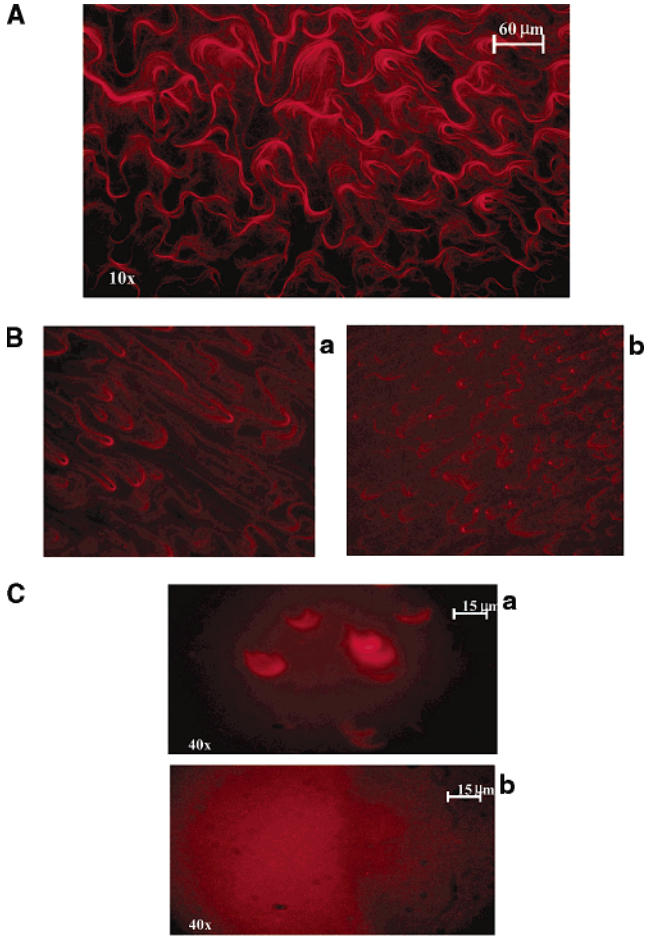

FIGURE 9: Comparison of the effects of HTI-286 and paclitaxel on fluorescently labeled microtubules. (A) Fluorescence micrographs of fluorescently labeled microtubules. Fluorescent microtubules, formed by combining unlabeled with 30% labeled tubulin in the presence of 10% glycerol at 35 °C, after 30 min of incubation were transferred to a slide before being imaged in the inverted microscope with an excitation filter of 570 nm. (B) Effect of paclitaxel on microtubules. Paclitaxel (45 μM) was added to the fluorescently labeled microtubules and the complex was incubated at 37 °C for 30 min (a) or at 4 °C for 30 min (b) prior to imaging. (C) Effect of HTI-286 on microtubules. HTI-286 (45 μM) was added to polymerized fluorescently labeled tubulin, and the resulting depolymerization was monitored at ambient temperature after 5 min (a) or at 37 °C for 10 min (b).

vancomycin in the presence of peptide ligand, it is evident that for such linked equilibria the enthalpy values change significantly with the concentration of vancomycin (*29*, *30*). Thus, the observed enthalpy of HTI-286 interactions with tubulin is associated primarily with the initial binding step. The large gain in enthalpy is due to potential contributions from the large number of bonding interactions (for example, hydrogen-bonding and van der Waals interactions) that occur between HTI-286 and tubulin. The unfavorable entropy is possibly due to loss of conformational flexibility of HTI-286 during the formation of the complex. In a recent calorimetric study of human immunodeficiency virus (HIV) gp120 interactions with CD4, it was shown that structural rearrangements in gp120 result in an unfavorable entropy component (*31*). In our CD spectroscopic studies, the results suggest that tubulin undergoes a change in the secondary structure due to the interactions with HTI-286. In the presence of HTI-286, the CD absorption of tubulin increased and the emission maximum of the tryptophan residues in

tubulin showed a hypsochromic shift. The blue shift in the emission spectrum of tubulin is consistent with a hydrophobic environment of the tryptophan residues in the inhibitor-bound form of the complex.

In contrast to the favorable enthalpic contributions associated with the binding event, the heat associated with the formation of tubulin ring was undetectable despite the opportunity to monitor the oligomer formation event separately. The absence of measurable heats during the tubulin oligomerization step is not surprising given the previously reported results from Timasheff's group (*15*) that tubulin association is entropically driven. In their studies on tubulin association (in the absence of any inhibitor), it was observed that the oligomerization is associated with endothermic heats and the magnitude of such changes is not large. In contrast to those studies, the heat released from the interactions of HTI-286 binding to tubulin is large and the entropic contribution is negative. Since HTI-286 binding to tubulin is causally linked to self-association of tubulin, conformational changes in tubulin (and possibly the inhibitor), and finally ring formation, it is conceivable that the net enthalpy change for these latter events is zero or that all events following the initial binding produce negligible changes in enthalpy. It is conceivable that the ring formation is driven primarily by a large entropic component consistent with the previous observations (*15*) following the initial binding events associated with the exothermic heats. The thermodynamics of the binding step is important for understanding structure−function relationships of HTI-286 analogues.

The observed difference in the stability of the tubulin oligomers formed in the presence of hemiasterlin and HTI-286 is intriguing. Both hemiasterlin and HTI-286 form the 1100 kDa oligomeric structure as seen by light scattering analyses. While the tubulin oligomer complex with hemiasterlin is stable, the HTI-286 complex is reversible under conditions of size-exclusion column chromatography. Thus, despite the similarity in the initial binding of HTI-286 and hemiasterlin to tubulin, the stability of the corresponding tubulin ring as well as the smaller oligomers is different. The differences in the stability of the tubulin rings and oligomers could result from the differences in the association and dissociation rate constants such that, the affinity of the two inhibitors is identical. Alternatively, the overall association constant for the formation of the tubulin rings may differ for the two inhibitors. The increased stability of the oligomers of the tubulin/hemiasterlin complexes are likely due to the chemical differences in the N-termini of the peptide, namely, indole vs the phenyl group in HTI-286, and their role in inducing intertubulin interactions. The tubulin size analysis experiments have unambiguously shown that HTI-286 and hemiasterlin A induce the formation of tubulin oligomers but not MTs, unlike other antitubulin agents such as discodermolide (or paclitaxel) that induce microtubule formation at low temperature in the absence of GTP or MAPs (*32*).

Recent photoaffinity labeling studies at Wyeth have shown that HTI-286 binding site overlap with the vinca and other peptide binding sites, based upon competition experiments in the presence of a benzophenone-modified analogue of HTI-286 (*33*) as photoaffinity label. However, the photoaffinity cross-linking occurred on α-tubulin rather than the *β*-subunit. Consistent with these findings, mutations in α-tubulin have been found in cells selected for resistance to HTI-286 (*34*). The binding site of HTI-286 on tubulin was also probed by use of the stilbene-modified analogue of HTI-286 in ultracentrifugation experiments. HTI-286 displaced the stilbene analogue from tubulin. Similarly, competition experiments between colchicine and the stilbene analogue were also carried out to determine if HTI-286 displaced colchicine from the tubulin binding site. Since colchicine and the stilbene analogue have distinct UV absorption profiles, their binding to tubulin was independently monitored at these wavelengths to determine if the binding sites are mutually exclusive. The lack of displacement of the stilbene analogue in the presence of colchicine supports the finding that the binding sites of the two inhibitors do not overlap.

HTI-286-Mediated Inhibition of Microtubules. The depolymerizing effects of HTI-286 (and hemiasterlin) on MTs are weak compared to the effects on tubulin monomer. Nearly stoichiometric levels of the inhibitors and, in absolute terms, high concentrations are necessary to reduce tubulin polymer mass as evidenced in the UV assays. Substoichiometric concentrations do not significantly depolymerize MTs, presumably due to weaker affinity of HTI-286 for the MTs. The weaker affinity could result from inaccessibility of the putative binding site in the polymerized form of the tubulin, although binding can occur to the ends with high affinity. It appears that HTI-286 does not alter the microtubule mass significantly at low concentrations. This result is reminiscent of the effects of other microtubule agents. For instance, it has been shown that antimicrotubule agents such as vinblastine do not depolymerize microtubules in cell cultures until the concentration of the antitubulin agent increases to the micromolar concentration range (*35, 36*). The affinity of HTI-286 for tubulin monomer is very high and therefore can alter the soluble pool of tubulin monomer at low concentrations due to the formation of tubulin oligomers. However, stoichiometric concentrations are necessary to completely depolymerize MTs. Therefore, it appears that the effects on soluble tubulin are much stronger than the depolymerizing effects on MTs. To our knowledge, this is the first time it has been shown that microtubules depolymerize to the 11-mer ring structures in the presence of stoichiometric levels of drug. The 11-mer ring corresponds to the discrete 18.5 S species observed in the ultracentrifugation experiments. The depolymerization event observed in the UV and fluorescence microscopy assays is very fast. The depolymerized microtubules do not enter the sizing column because the tubulin is still a large polymer. However, after prolonged incubation of these polymers in the presence of stoichiometric concentrations of HTI-286, the 11-mer structures are formed and are readily detected in the sizing column by the light scattering detector. Since the smaller oligomers form very slowly from MTs and rapidly from soluble tubulin, we hypothesize that HTI-286 binding to microtubule induces formation of the oligomer via transient formation of the monomeric tubulin, for which the binding affinity is very high. Alternatively, it is also possible that the closed ring structures form by peeling away the protofilament from the MTs. The proposed dual mode of action on tubulin is summarized in Scheme 1. Since the initial binding of HTI-286 to tubulin is very tight, the macroscopic quantity K_D-(overall), which is a product of the individual association equilibria (represented as K_1, K_2, etc) of the tubulin complex

Scheme 1

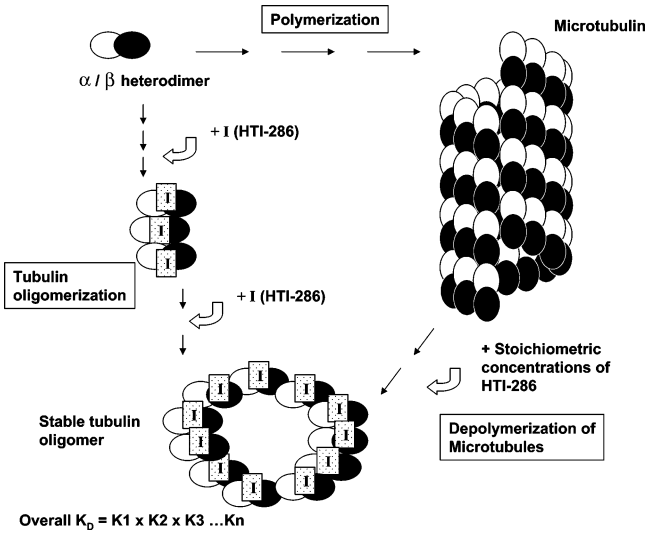

is likely to be even tighter. Therefore, very low concentrations of the inhibitor may be sufficient to convert monomeric tubulin to a functionally inactive state resulting from tubulin association. The results described in this work also demonstrate that HTI-286 binds MTs, although the depolymerizing effects are evident primarily at the higher concentrations. In contrast, the effects of HTI-286 on association of tubulin occur at substoichiometric concentrations. HTI-286 can accumulate within the cell due to high-affinity binding to tubulin and also due to its resistance to drug export mechanism(s) (*10*, *11*), thereby increasing the intracellular concentration to potentially stoichiometric levels to alter the stability of microtubules. In conclusion, our studies suggest that HTI-286 can potentially alter the MT dynamics in the normal cell cycle by binding and destabilizing microtubules and also by lowering the pool of soluble tubulin monomers.

ACKNOWLEDGMENT

We thank Drs. Michael Brenowitz (Albert Einstein College of Medicine) and Tom Laue (University of New Hampshire) for providing comments on the manuscript and Dr. George Na (Wyeth) for his suggestions on the use of ultracentrifugation technique.

REFERENCES

1. Hamel, E. (1996) *Med. Res. Rev. 316*, 207−231.
2. Downing, K. H. (2000) *Annu. Rev. Cell. Dev. Biol. 16*, 89−111.
3. Timasheff, S. N., Andreau, J. M., and Na, G. C. (1992) *Pharmacol. Ther*. *52*, 191−210.
4. Correia, J. J., and Lobert, S. (2001) *Curr. Pharm. Des. 7*, 1214−1228.
5. Nogales, E., Whittaker, M., Milligan, R. A., and Downing, K. H. (1999) *Cell 96*, 79−88.
6. Margolis, R. L., and Wilson, L. (1978*) Cell 13*, 1−8.
7. Margolis, R. L., and Wilson, L. (1998) *Bioessays 20*, 830−836.
8. Anderson, H. J., Coleman, J. E., Andersen, R. J., and Roberge, M. (1995) *Cancer Chemother. Pharmacol. 39*, 223−226.
9. Zask, A., Birnberg, G., Cheung, K., Cole, K., Kaplan, J., Niu, C., Norton, E., Sandanayaka, V., Suayan, R., Tan, Z., Yamashita, A., Loanzo, F., Beyer, C., Discafani, C., Greenberger, L. M., and Ayral-Kaloustian, S. (2002) *Proc. Am. Assoc. Cancer Res*., abstr. 3653.
10. Loganzo, F., Discafani, C., Annable, T., Beyer, C., Musto, S., Hardy, C., Hernandez, R., Baxter, M., Ayral-Kaloustian, S., Zask, A., Singanallore, T., Khafizova, G., Nieman, J., Andersen, R. J., and Greenberger, L. M. (2002) *Proc. Am. Assoc. Cancer Res*., abstr. 1316.
11. Loganzo, F., Discafani, C. M., Annable, T., Beyer, C., Musto, S., Hari, M., Tan, X., Hardy, C., Hernandez, R., Baxter, M., Singanallore, T., Khafinoza, G., Poruchynsky, M. S., Fojo, T., Nieman, J. A., Ayral-Kaloustian, S., Zask, A., Andersen, R. J., and Greenberger, L. (2003) *Cancer Res. 63*, 1838−1845.
12. Bai, R., Taylor, G. F., Schmidt, J. M., Williams, M. D., Kepler, J. A., Pettit, G. R., and Hamel, E. (1995) *Mol. Pharmacol. 47*, 965−976.
13. Panda, D., Anantharaman, V., Larson, G., Shih, C., Jordan, M. A., and Wilson, L. (2000) *Biochemistry 39*, 14121−14127.
14. Perez-Ramirez, B., Andreu, J. M., Gorbunoff, M. J., and Timasheff, S. N. (1996) *Biochemistry 35*, 3277−3285.
15. Frigon, R. P., and Timasheff, S. N. (1975) *Biochemistry 14*, 4567−4573.
16. Lobert, S., Frankfurter, A., and Correia, J. J. (1995) *Biochemistry 34*, 8050−8060.
17. Andersen, R. J., Coleman, J. E., Piers, E., and Wallace, D. (1997) *Tetrahedron Lett. 38*, 317−320.
18. Andersen, R., Piers, E., Nieman, J., Coleman, J., and Roberge, M. WO 99/32509.
19. Wyatt, P. J. (1993) *Anal. Chim. Acta 272*, 1−40.
20. Schuck, P. (2000) *Biophys. J. 78*, 1606−1619.
21. Laue, T. M., Shah, B. D., Ridgeway, T. M., and Pelletier, S. L. (1992) in *Analytical Ultracentrifugation in Biochemistry and Polymer Science* (Harding, S. E., Rowe, A. J., and Horton, J. C., Eds.) pp 90−125, Royal Society of Chemistry, Cambridge, U.K.
22. Jamieson, E. R., Jacoson, M. P., Barnes, C. M., Chow, C. S., and Lippard, S. J. (1999) *J. Biol. Chem. 274*, 12346−12354.
23. Lobert, S., Frankfurter, A., and Correia, J. J. (1995) *Biochemistry 34*, 8050−8060.
24. Shearwin, K. E., and Timasheff, S. N. (1992) *Biochemistry 31*, 8080−8089.
25. Barbier, P., Gregoire, C., Devred, F., Sarrazin, M., and Peyrot, V. (2001) *Biochemistry 40*, 13510−13519.
26. Singer, W. D., Hersh, R. T., and Himes, R. H. (1988) *Biochem. Pharmacol. 37*, 2691−2696.
27. Bai, R., Neil, D., Sackett, D. L., and Hamel, E. (1999) *Biochemistry 38*, 14302−14310.
28. Andreu, J. M., and Timasheff, S. N. (1981) *Arch. Biochem. Biophys. 211*, 151−157.
29. McPhail, D., and Cooper, A. (1997) *J. Chem. Soc., Faraday Trans. 93*, 2283−2289.
30. Cooper, A., and McAuley-Hecht, K. E. (1993) *Philos. Trans. R. Soc. London 345*, 23−25.
31. Myszka, D. G., Sweet, R. W., Hensley, P., Brigham-Burke, M., Kwong, P. D., Hendrickson, W. A., Wyatt, R., Sodroski, J., and Doyle, M. L. (2000) *Proc. Natl. Acad. Sci. U.S.A. 97*, 9026−9031.
32. ter Haar, E., Kowalski, R. J., Hamel, E., Lin, C. M., Longley, R. E., Gunasekara, S. P., Rosenkranz, H. S., and Day, B. W. (1996) *Biochemistry 35*, 243−250.
33. Nunes, M., Kaplan, J., Loganzo, F., Zask, A., Ayral-Kaloustian, S., and Greenberger, L. M. (2002) *Eur. J. Cancer 38*, S119.
34. Poruchynsky, M. S., Annable, T., Kim, J.-H., Fojo, T., and Greenberger, L. M. (2001) *Clin. Cancer Res. 7*, 3810s.
35. Singer, W. D., Jordan, M. A., Wilson, L., and Himes, R. H. (1989) *Mol. Pharmacol. 36*, 366−370.
36. Jordan, M. A., Thrower, D., and Wilson, L. (1991) *Cancer Res. 51*, 2212−2222.

BI035530X